Food Chemistry 396 (2022) 133493

Contents lists available at ScienceDirect

Food Chemistry

journal homepage: www.elsevier.com/locate/foodchem

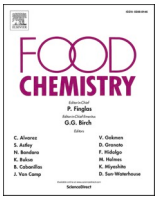

# Valorization of brewer's spent grain by consecutive supercritical carbon dioxide extraction and enzymatic hydrolysis

Patricia Alonso-Riaño, Rodrigo Melgosa, Ester Trigueros, Alba Ester Illera, Sagrario Beltrán, M. Teresa Sanz *

*Department of Biotechnology and Food Science, University of Burgos, Plaza Misael Bañuelos s/n, 09001 Burgos, Spain*

ARTICLE INFO

*Keywords:*
Biorefinery
Brewer's spent grain
Supercritical fluid extraction
Enzymatic hydrolysis

ABSTRACT

The double effect of supercritical carbon dioxide, sc-$CO_2$, in a biorefinery concept applied to brewer's spent grain (BSG) was assessed in this work. Extraction conditions to remove and valorize the lipophilic fraction were studied (20–40 MPa and 40–80 °C) obtaining a maximum yield of 5.70 ± 0.07 g/100 $g_{BSG}$ at 80 °C and 40 MPa. High pressures and temperatures resulted in higher content of total phenolic and flavonoid compounds, as well as higher antioxidant capacity. It was observed an improvement of the enzymatic hydrolysis yield by cellulase in the sc-$CO_2$ treated BSG compared to the non-treated. This improvement could be partially attributed to the removal of the lipid fraction and to morphological changes of BSG after sc-$CO_2$. Based on this double benefit, sc-$CO_2$ can play an important role on biomass valorization.

## 1. Introduction

Renewable resources constitute the basis of the development of a bioeconomy-based society. The implementation of a bioeconomy involves strategies based on biorefinery technologies to improve the use of these biological resources. Therefore, biorefineries constitute a key pillar to close material loops offering a wide variety of products from different types of biomass to boost emerging circular economy extending the life cycle of a product (Manzanares, 2020).

Integration of waste material flows as raw material to another industrial process is one of the main principles of the circular economy to reach the zero-waste objective. The selection of the raw material is one of the basis for the technology and economic successful implementation of the bio-economy. In this regard, lignocellulosic biomass is the renewable resource that can be considered the pillar for a sustainable development. The brewing industry generates different solid by-products during processing, being the most important the brewer's spent grains (BSG). BSG is the solid residue generated after the mashing and wort filtration process. It accounts to about 85% of the total byproducts, being generated approximately 20 kg per 100 L (Kitryte et al., 2015). BSG is mainly used for animal feed (70%), biogas production (10%), or disposed of in landfills. However, BSG presents a valuable chemical composition with a high content of protein and carbohydrates and an important source of phenolic compounds. BSG also contains an important amount of lipids (5%) with more than 50% of linoleic acid (Fărcaş et al., 2015). The integration of BSG within a holistic approach to produce different bioproducts will have a great social and economic impact also at local level (Manzanares, 2020) due to the expansion and growth of craft and microbreweries at local and regional level in the last decades.

Biorefinery development also involves new and optimized technologies for the conversion of biomass materials into bio-based commodities (Manzanares, 2020). Due to the chemical composition of the BSG, different techniques have been proposed to valorize this lignocellulosic biomass, such as enzymatic, acid and basic hydrolysis, ultrasound assisted extraction or microwave assisted extraction (Ferrentino et al., 2019).

High pressure processing of biomass offers a great possibility to extract and valorize the different bioactive components. Among the different high pressure processes, the use of $CO_2$ in its supercritical state (sc-$CO_2$) has become a promising technology to process biomass. At supercritical conditions ($T_c = 31.1$ °C $p_c = 7.39$ MPa), $CO_2$ presents gas-like (high diffusivities) and liquid-like (good solvation power) properties. sc-$CO_2$ has been extensively studied as a green extracting agent over traditional organic extraction solvents to valorize different biomass components (Arshadi et al., 2016). Furthermore, the energy demand to get $CO_2$ in its supercritical state is lower than for other solvents and leaves no solvent residue allowing the direct downstream processing of

* Corresponding author.
*E-mail address:* tersanz@ubu.es (M.T. Sanz).

https://doi.org/10.1016/j.foodchem.2022.133493
Received 9 November 2021; Received in revised form 13 June 2022; Accepted 13 June 2022
Available online 15 June 2022

the raffinate avoiding the solvent removal step which is time-consuming and energy-intensive. The easy recovery of the solvent enables to re-use of $CO_2$ after the process. Therefore, the choice of sc-$CO_2$ extraction is an ideal initial step in a biorefinery process being also environmentally sustainable allowing to use $CO_2$ as a resource.

When dealing with sc-$CO_2$ treatment of biomass from a biorefinery perspective, the focus must be not only on extraction but also on the effect of sc-$CO_2$ on the residual biomass after extraction that could lead to enhanced yields of other products. $CO_2$ at supercritical conditions can penetrate into the small pores of the lignocellulosic biomass resulting in structural modifications. Furthermore, $CO_2$ can be quickly released during the depressurization process, leading to explosion decompression of the feedstock promoting a decrease in its crystallinity. These structural changes result in a larger exposed surface area of the polymers such as glucans and xylans to hydrolytic enzymes (Morais et al., 2015). In this regard, a future perspective of advanced biorefinery systems must consider the combination of one or more of different approaches and technologies. In this work, an integrated process is proposed by combining sc-$CO_2$ treatment for extracting the lipid fraction of BSG with a subsequent enzymatic hydrolysis step of the remaining biomass to achieve a holistic approach to obtain a wide range of products from BSG.

In literature, it is also reported that $CO_2$ can be solubilized in the moisture content of the biomass leading to the formation of carbonic acid promoting hydrolysis of biomass polymers such as hemicelluloses (Arshadi et al., 2016). However, these studies were carried out under more severe conditions of temperature (120–180 °C) where dissolved $CO_2$ improves the autocatalytic effect of water in subcritical conditions. These studies concluded that temperature, moisture and the presence of $CO_2$ were the most important processing parameters to obtain a high yield of hemicellulose removal (Aguirre-Fierro et al., 2020; Morais et al., 2014; Relvas et al., 2015) that has been demonstrated to lead to high enzymatic saccharification yield of the remaining cellulose in the biomass (Aguirre-Fierro et al., 2020). However, the focus of this work is to check if common temperatures used in sc-$CO_2$ extraction (lower than 100 °C) and low moisture content in the feedstock somewhat enhances glucose yield by enzymatic hydrolysis after sc-$CO_2$ extraction of the oily fraction of BSG, which up to the authors' knowledge, has not been reported in the literature.

The enzymatic hydrolysis of the reaming polysaccharide fraction after sc-$CO_2$ treatment, at conditions usually employed for lipid extraction, into monomeric sugars will be monitored by comparing the sugar yields of untreated and sc-$CO_2$ treated BSG. This green approach based on GRAS solvents offers high potential for sustainable biomass valorisation. Due to the properties of sc-$CO_2$ as green solvent for natural compounds, a complete study of the extraction of BSG lipophilic fraction by sc-$CO_2$ was also carried out.

Regarding the extraction of lipophilic components from BSG by sc-$CO_2$, some previous studies can be found in the literature (Fernández et al., 2008; Ferrentino et al., 2019; Kitryte et al., 2015; Spinelli et al., 2016). These works covered a maximum operating pressure of 300–350 bar. At this maximum pressure level, an increase in temperature resulted in a decrease in the extraction yield due to dominant effect of decreasing sc-$CO_2$ density with temperature over an increase of solute vapor pressure. Therefore, in this work, higher extraction pressures were explored to check a crossover point with pressure previously reported for other oil vegetable at pressures higher than 40 MPa where solute vapor pressure increase with temperature is the dominant effect (Rebolleda et al., 2013). In this work, extraction kinetics at different pressures, temperatures and milling degree were performed to determine the optimum operating conditions, covering a wider pressure and temperature range than the extraction conditions previously reported in literature. Extraction kinetics were conveniently modelled by Sovova's model (Sovová, 2005). Mathematical modelling is of great importance in modern food engineering. Knowledge of dependence of model parameters on process conditions helps to optimization, simulation design and control of process (Bucić-Kojić et al., 2013). Characterization of the oily fraction in terms of fatty acid profile and bioactive compounds composition for the different extracts was also done. It was determined the effect of the sc-$CO_2$ treatment on subsequent sugar yield by enzymatic hydrolysis. Changes were assesed by X-ray diffraction, chemical composition and surface structures analysis. Therefore, valorization of BSG is presented under a biorefinery integration concept.

## 2. Experimental section

### 2.1. Materials

The raw material used in this work was the brewer's spent grain supplied by Brebajes del Norte, S.L. (Dolina craft beer, Burgos, Spain) with an average moisture content of 70–80% (w/w). This raw material was first preconditioned, as soon as obtained, by washing with water until no turbidity was observed and drying it in an air convection oven until reaching a final moisture content of 8.5% (w/w). Dehydration is necessary to reduce the storage and transportation costs as well as to reduce the microbial spoilage.

Biomass characterization was performed according to the NREL protocols. Previous details about BSG chemical characterization can be found elsewhere (Alonso-Riaño et al., 2021). Carbohydrates were quantified by high-performance liquid chromatography (HPLC) with a Bio-Rad Aminex-HPX-87 H column, a variable wavelength detector (VWD) and a refractive index detector (RID) using a mobile phase constituted by 0.005 M sulphuric acid. The column and the refractive index detector were maintained at 40 °C. The oil content of the BSG was determined by Soxhlet extraction (Buchi B-8111) using hexane as solvent, resulting to be 5.92 ± 0.01 (w/w, %) in a dry basis. The dry BSG was milled in a Retsch SM100 mill to get two types of final fineness by using bottom sieves with aperture sizes of 500 μm and 1000 μm. Particle size distribution for each of the aperture sizes of the sieves was determined by a vibratory sieve shaker (CISA, RP.09) presenting the following distribution in percentage (w/w): (1) fineness of 1000 μm: >1000 μm, 14.2%; 1000–500 μm, 58.1%; 500–250 μm, 17.4%; 250–125 μm, 6.5% and <125 μm, 3.9% (2) fineness of 500 μm: >1000 μm, 0%; 1000–500 μm, 2.9%; 500–250 μm, 70.4%; 250–125 μm, 21.0% and <125 μm, 5.7%.

The hydrolytic enzyme used in this work was a cellulase, 1,4-(1,3:1,4)-β-D-Glucan 4-glucanohydrolase, EC 3.2.1.4, from *Aspergillus niger* provided by Sigma-Aldrich. The enzyme units, as reported by the supplier was 1.18 U/mg, being 1 U the corresponding amount of enzyme that liberates 1 μmol of glucose from carboxymethyl cellulose per minute at pH of 5.0 and 37 °C.

### 2.2. Supercritical fluid extraction equipment and procedure

The sc-$CO_2$ extraction experiments were carried out in a laboratory SFE-plant whose P&I diagram has been previously described (Benito-Román et al., 2018). In a SFE experiment, 8.5 g of dry BSG were loaded in the extractor (26.5 mL capacity, with ½" internal diameter). Two syringe pumps (ISCO 260 DM), that work alternatively, provide an uninterrupted flow of $CO_2$ (Carburos metálicos, liquid $CO_2 \geq$ 99.9%) compressed up to the desired operating working pressure. The pressurized solvent was pre-heated up to the desired extraction temperature before entering the extractor. The extractor was held in an oven whose temperature is controlled within an accuracy of ±0.5 °C. The extraction yield was determined gravimetrically by measuring the extract weight at different time intervals.

The first group of SFE experiments were carried out to determine the effect of particle size at constant operation pressure and temperature of 30 MPa and 40 °C, respectively. First, unsieved and unmilled BSG was used. Subsequently, different particle sizes were studied according to the fineness particle distribution obtained by milling and sieving by using bottom sieves with aperture sizes of 1000 and 500 μm. Then, 8.5 g of BSG were charged in the extractor according to the percentage and

particle size distribution found for each type of final fineness reported in section 2.1. This way, the effect of particle size was studied, avoiding the effect of chemical composition of each particle size fraction. Once the final fineness was selected, the effect of pressure, from 20 to 40 MPa, and temperature, from 40 to 80 °C, was assessed.

### 2.3. Enzymatic hydrolysis

Enzymatic hydrolysis was performed on samples after sc-$CO_2$ treatment and non-treated BSG samples. Enzymatic hydrolysis was carried out at 50 °C in an acetate buffer at pH = 5. The cellulase concentration, expressed as enzyme:BSG ratio (w/w), was varied in the mass percent range from 0.25% to 1%. Samples were withdrawn at regular time intervals to plot the corresponding hydrolysis curves. To stop the hydrolytic reaction, the enzyme was inactivated by heating the withdrawn samples at 100 °C for 5 min and immediately cooling in ice and kept in the refrigerator until analysis.

Liquid samples were analyzed by HPLC for determination of monomeric sugar concentration (glucose, xylose and arabinose) according to the method described in section 2.1 for carbohydrate indentification in the raw material.

### 2.4. Analytical methods

#### 2.4.1. Determination and quantification of fatty acids profile

The fatty acids profile was determined by the AOAC method (AOAC, 1997). The fatty acid methyl esters were firstly prepared and then analyzed by gas chromatography (GC) in a Hewlett Packard gas chromatograph (6890N Network GC System) equipped with an auto-sampler (7683B series) and a flame ionization detector (FID). The method has been previously described in detail (Rebolleda et al., 2012). Fatty acid methyl esters were identified by comparison of their retention times with those of chromatographic standards (Sigma Chemical Co.). Their quantification was made by relating the peaks area to the area of an internal standard (methyl tricosanoate). Calibration curves were made for several pairs formed by the internal standard + several representative chromatographic standards in order to find the corresponding response factors. Results were expressed as mg of fatty acid per g of extract and as fatty acid percentage.

#### 2.4.2. Determination of total phenolic compounds

The total phenolic content of sc-$CO_2$ extracts was determined by the Folin-Ciocalteu method (Singleton et al., 1999). The sc-$CO_2$ extract was diluted in ethanol (5 mg/mL). Briefly, 500 μL of the diluted extract were mixed with 5.0 mL of water and then, 500 μL of the Folin-Ciocalteu reagent. After that, 1 mL of sodium carbonate 7.5% (w/v) was added to the mixture. Sample was filtered and centrifuged and the the absorbance of optically clear supernatant was measured at 725 nm after 60 min of reaction in darkness (spectrophotometer V-750, Jasco, Japan). A calibration curve was prepared with standard solutions of gallic acid and results were expressed as mg of gallic acid equivalent (GAE)/g extract (mg GAE/$g_E$).

#### 2.4.3. Determination of total flavonoid compounds

The total flavonoid content (TFC) was determined by the aluminum trichloride method as described by Spinelli et al. (2016) with slight modifications. An ethanolic solution was prepared by dissolving 5 mg of the sc-$CO_2$ extract in 1 mL of ethanol. After that, 0.5 mL of this solution were mixed with 2.0 mL of distilled water and 0.15 mL of $NaNO_2$ (5% w/v). Subsequently (after 6 min), 0.15 mL of $AlCl_3$ solution (10%, w/v) were added. Finally, after 5 min reaction, 1 mL of NaOH (1 M) and 1.2 mL of ethanol were added to the mixture. After 30 min in darkness, sample was filtered and centrifuged and the the absorbance of optically clear supernatant was measured at 415 nm. A quercetin standard curve was constructed to express the results as mg of Quercetin Equivalent per gram of extract, mg QE/$g_E$.

#### 2.4.4. Determination of antioxidant capacity

The antioxidant activity of the sc-$CO_2$ extracts was assesed by the ABTS method. This method is based on the decolorization of the radical cation 2,2′-azinobis-(3-ethylbenzothiazoline-6-sulfonic acid) ($ABTS^+$) prepared according to Re et al. (1999). Briefly, 3 mL of the $ABTS^+$ solution were mixed with 1 mL of the BSG oil diluted in ethanol (5 mg/mL). After 1 h in the dark, sample was filtered and centrifuged and the the absorbance of optically clear supernatant was measured at 734 nm and 25 °C using ethanol as a blank. A Trolox standard curve in ethanol was used to express the antioxidant capacity of the samples as mg of Trolox Equivalent (TE) per g of extract (mg TE/$g_E$).

#### 2.4.5. Determination of individual phenolic compounds

The identification and quantification of individual phenolic compounds was performed according to the method previously applied by Alonso-Riaño et al. (Alonso-Riaño et al., 2021; Alonso-Riaño et al., 2020). The sample was filtered through a 0.2 μm syringe filters and injected in the HPLC system. The separation was performed at 25 °C on a Kinetex® μm Biphenyl 100 Å, 250 × 4.6 mm column (Phenomenex). The mobile phase consisted of ammonium acetate 5 mM with acetic acid (1%; v/v) in water (solvent A) and ammonium acetate 5 mM with acetic acid (1%; v/v) in acetonitrile (solvent B). Further details have been previously described (Alonso-Riaño et al., 2021). The HP ChemStation software was employed to collect and analyse the chromatographic data delivered by the diode array detector and own library was used to identify the different phenolic compounds by comparing retention times and spectral data with those of authentic standards: vanillin, p-coumaric acid and ferulic acid (Sigma-Aldrich). Individual stock solutions of the above phenolic compounds, and their mixtures, were prepared in methanol to plot the calibration curves.

#### 2.4.6. X-ray diffraction (XRD)

An X-ray diffractometer (Bruker D8 Discover, Davinci Design) was used to determine the crystallinity of the different BSG samples: untreated BSG, sc-$CO_2$-treated BSG and after enzymatic hydrolysis of the BSG samples. A scan type of theta-2-theta with a step size of 0.05 was carried out at 0.05/min. The scattering angle (2θ) was varied from 5 to 70°.

#### 2.4.7. Scanning electron microscopy (SEM)

The surface morphology of the different samples was examined in a Scanning Electron Microscope JEOL JSM-6460LV with Energy Dispersive X-ray (JEOL Ltd. Japan) operating at 20 kV. Samples were gold-sputtered and observed at different magnifications.

### 2.5. Modelling

#### 2.5.1. Supercritical fluid extraction modelling

The model proposed by Sovová was used to fit the experimental extraction curves (Sovová, 2005). This type of model has been successfully used to describe the extractive curves of different seed oils (Benito-Román et al., 2018; Rebolleda et al., 2012, 2013). In the model of Sovová the extraction yield is expressed as:

$$e = \frac{E}{N_m} \quad (1)$$

where E is the amount of extract (kg) and $N_m$ the amount of insoluble solid (kg) loaded in the extractor. The amount of solvent consumed is obtained by:

$$q = \frac{\dot{Q}\, t}{N_m} \quad (2)$$

where $\dot{Q}$ is the solvent flow rate (kg/s) and t the extraction time (s). This model considers that the extraction curves consist of two parts. First, the easily accessible solute from broken cells is transferred directly to the

fluid phase and in the second part of the extraction curve, the solute from intact cells diffuses first to broken cells and then to the fluid phase. For vegetable oil extraction, Sovová found that extraction curves are initially linear with a slope close to the value of oil solubility in $CO_2$ (Sovová, 2005). Assuming an initial solubility control in the first part of the extraction curve, Sovová proposed Eqs. (3) and (4) to evaluate the first and second part of the extraction curve, respectively:

$$e = q\,y_s, \text{ for } 0 \le q \le q_c \tag{3}$$

$$e = x_u[1 - C_1\exp(C_2 q)], \quad \text{for } q > q_c \tag{4}$$

$C_1$ and $C_2$ are adjustable parameters, $y_s$ is the experimental solubility datum, $q_c$ the crossing point and $x_u$ is the solute concentration in the BSG (kg solute/kg insoluble solid). The adjustable parameters of the model were calculated by using the software Statgraphics Centurion XVI X64 and the Marquardt's algorithm. From constants $C_1$, $C_2$ the co-ordinate $q_c$ at the crossing point, and the bed porosity (ε), the volumetric fraction of broken cells in the particles, called grinding efficiency, r, and the solid-phase mass transfer coefficient, $k_s a_s$, can be estimated (Sovová, 2005):

$$r = 1 - C_1\exp(-C_2 q_c/2) \tag{5}$$

$$k_s a_s = (1 - r)(1 - \varepsilon)\dot{Q}C_2/N_m \tag{6}$$

*2.5.2. Enzymatic hydrolysis modelling*

The experimental enzymatic hydrolysis data were fitted to the hyperbolic correlation of Holtzapple, which involves two kinetic parameters ($C_{i,max}$ and $t_{1/2}$) (Holtzapple et al., 1984):

$$C_i = \frac{C_{i,max} \cdot t}{t_{1/2} + t} \tag{7}$$

where $C_i$ is the concentration of a monomeric sugar (glucose, xylose or arabinose), $C_{i,max}$ is the maximum concentration of the monomeric sugar that could be achieved at the working experimental conditions, $t_{1/2}$ is the time required to achieved 50% of $C_{i,max}$ and t is the enzymatic hydrolysis time (min). To estimate the kinetic parameters, non-linear regression was performed by using the Marquardt algorithm (Statgraphics Centurion XVI X64).

*2.6. Statistical analysis*

Statistical analyses were conducted using the software Statgraphics Centurion XVI X64. The results were presented as a mean ± standard deviation of at least three replicates. To confirm significant differences, the Fisher's least significant differences method at p-value ≤ 0.05 was applied.

## 3. Results and discussion

*3.1. Supercritical extraction of the lipophilic fraction of BSG*

The first step in the BSG valorisation within a biorefinery concept was the extraction of the valuable lipophilic fraction of the BSG. Extraction curves were obtained and the optimal conditions required to achieve the maximum extraction yield were determined.

*3.1.1. Influence of process parameters*

Fig. 1 shows the extraction curves at 30 MPa and 40 °C obtained for non-ground BSG and two final fineness obtained for 1000 and 500 μm sieve sizes in the mill. From the extraction curves it can be observed that the initial extraction rate increased by decreasing the particle size. This could be due to the higher amount of compounds that can be easily extracted outside the particle at smaller particle sizes that would reduce the importance of diffusion compared to convection (Rebolleda et al., 2013). Furthermore, lower extraction yields, for a given extraction time, were obtained with larger particle size distribution, since only part of the oil contained in the largest particles seems to be accessible to sc-$CO_2$ as a result of internal diffusional limitations. Therefore, for further experiments, BSG was charged in the extraction according to the particle size distribution obtained for a fineness obtained with the 500 μm sieve size in the mill to study the effect of pressure and temperature.

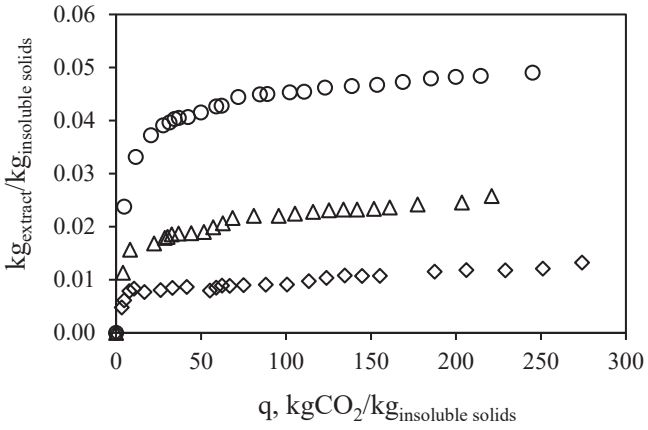


**Fig. 1.** Effect of the particle size on the extraction kinetics of oil from BSG at 30 MPa and 40 °C: original BSG (◇), and different PSD for fineness obtained with different sieve size in the mill (1000 μm (△), 500 μm (○)).

The effect of extraction temperature was studied at 40, 60 and 80 °C, at three different pressure levels, 20, 30 and 40 MPa. At any of the operating temperatures, an increase in the extraction rate was observed when pressure was increased (see Fig. 2). This behavior can be attributed to the higher solvating power associated to the higher $CO_2$ density. Fernandez et al. (2008) observed also an increase in the extraction rate with pressure from 10 to 35 MPa, at a constant temperature of 40 °C. However, these authors reported lower extraction yields with a highest value of 3.5 g extract per 100 g of BSG, probably due to the use of partially dried BSG by vacuum drying, with a moisture content of 58% (w/w) and a larger mean particle size of 0.85 mm of the BSG. At the best extraction conditions reported by Fernandez et al. (40 °C and 35 MPa), Kitryté (2015) reported a similar extraction yield as the one obtained in this work (5.49 ± 0.07 g /100 $g_{BSG}$) by using freeze-dried BSG samples of 0.2 mm mean particle size. In the present work a maximum extraction yield of 5.70 ± 0.07 g /100 $g_{BSG}$ at 80 °C and 40 MPa was obtained.

Regarding the effect of temperature at constant pressure, different behavior was observed at the different pressures studied in this work. At the lowest pressure, 20 MPa, an increase in temperature resulted in a decrease in the extraction rate. This trend was also observed by Fernandez et al. (2008) in the pressure range from 10 to 30 MPa and temperature range from 40 to 80 °C. However, at the highest pressure essayed in this work, 40 MPa, an increase in temperature led to an increase in the extraction rate. As it is well described in literature (Rebolleda et al., 2013), temperature has two opposite effects that influence sc-$CO_2$ extraction. As temperature increases, the solute vapor pressure of the extract increases, increasing its solubility, but the solvent density decreases, decreasing the solvent power of sc-$CO_2$. The results obtained in this work indicated that the first effect prevails at high pressures and the second at low pressures. At 40 MPa, the increase of vapor pressure with temperature compensates the effect of a lower sc-$CO_2$ density in the extraction rate. These results agree with literature (Rebolleda et al., 2012) that reported an increase of seed oil solubility with temperature when extraction was carried out at pressures higher than 40 MPa, pressure at which a crossover behavior is usually observed in vegetable oils. This crossover point has been reported for the first time for BSG oily fraction extraction by sc-$CO_2$, according to the authors's knowledge.

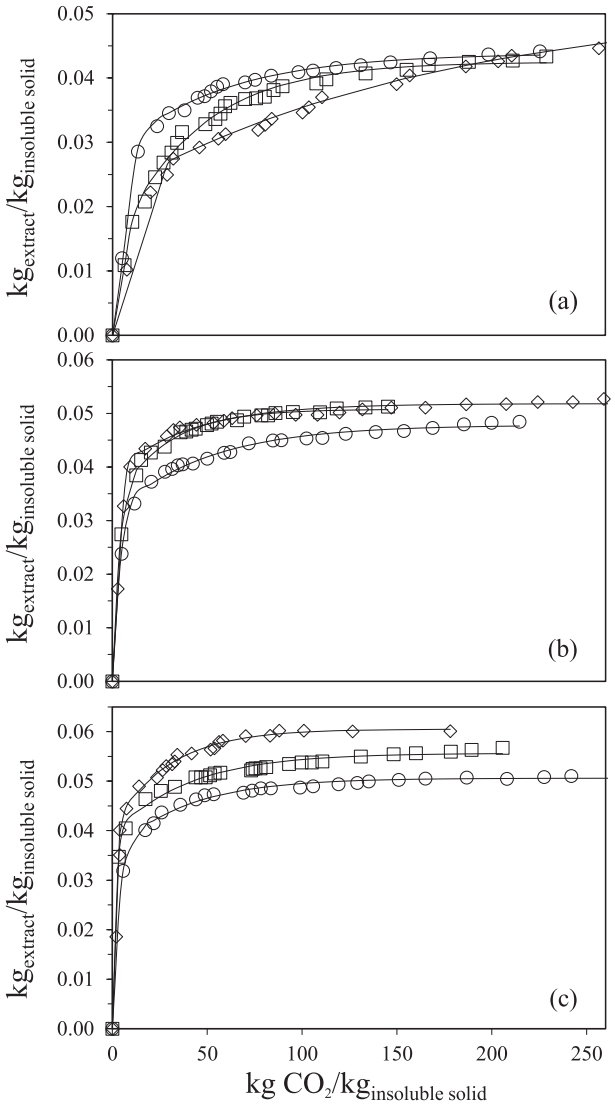


**Fig. 2.** Effect of operating temperature and pressure on extraction kinetics of oil from BSG: (a) 20 MPa (b) 30 MPa (c) 40 MPa: (○) 40 °C (□) 60 °C (◇) 80 °C. Continuous lines represent the Sovová's model.

### 3.1.2. Modeling of the supercritical fluid extraction

According to the model proposed by Sovová et al (2005) and described in section 2.5.1, for many vegetable oil, the extraction curves are initially linear with a slope close to the value of oil solubility in sc-$CO_2$ at the working conditions. To check if the initial slopes of the extraction curves are within the range of previously reported vegetable oil solubility, the initial slope was evaluated and compared with the general equation proposed by Del Valle et al. (2012) to predict the solubility of vegetable oils in high-pressure $CO_2$ (within ± of experimental values) as a function of $CO_2$ density and temperature:

$$c_{sat}\left(g{\cdot}kg^{-1}\right) = 8.07\left(\frac{\rho}{910}\right)^{\left[9.59-8.45\left(\frac{\rho}{910}-1\right)-23.0\left(\frac{\rho}{910}-1\right)^{2}\right]}\exp\left\{-4182\left[1-259\left(\frac{1}{T}-\frac{1}{313}\right)\right]\left(\frac{1}{T}-\frac{1}{313}\right)\right\} \quad (8)$$

where $CO_2$ density, ρ, and temperature, T, are expressed as kg/m$^3$ and K, respectively.

According to Del Valle et al. (2012) Eq. (8) can be applied to systems composed by pure oil + high-pressure $CO_2$ as well as to oil contained in different vegetable substrates, since the initial stages of the extraction process are typically solubility-controlled. To correct the values obtained at temperatures different from 40 °C (313.15 K), the initial slopes were divided by the temperature-correction term (TCT) (Del Valle et al., 2012):

$$TCT = \exp\left\{-4182\left[1-259\left(\frac{1}{T}-\frac{1}{313}\right)\right]\left(\frac{1}{T}-\frac{1}{313}\right)\right\} \quad (9)$$

The corrected initial extraction slopes have been plotted in Fig. S1 as a function of pure $CO_2$ density, together with the prediction of the oil solubility and the error limit from the General Model. It can be concluded that the values of the slope of the first part of the extraction curves are within the error limits for solubility of vegetable oils in $CO_2$. Therefore, it can be assumed that the initial part of the extraction curves is solubility-controlled and the Eqs. (3) and (4) can be used to fit the extractive curves.

Fernández et al. (2008) reported solubility data for BSG extraction by sc-$CO_2$ based on the dynamic flow criteria. These values have not been plotted in Fig. S1 since they are much lower than the values obtained in the present work. For instance at 30 MPa and 40 °C, these authors reported values of 0.4581 mg/g $CO_2$ (or g/kg $CO_2$), while in this work the solubility value determined according to the initial slope of the extraction curve was one order of magnitud higher which agrees with previous solubility data of vegetable oils in sc-$CO_2$.

The adjustable parameters of Sovova's model have been listed in Table S1 toghether with the volumetric fraction of broken cells in the particles, r, and the solid-phase mass transfer coefficient, $k_sa_s$, evaluated from the model parameters (Eqs. (5) and (6)). The calculated extraction curves are plotted in Fig. 2 where a good agreement can be observed between experimental data and model fitting. The quality of the fitting has been evaluated through the values of the Root Mean Square Deviation (RMSD) between experimental and calculated extraction yields:

$$RMSD = \sqrt{\frac{\sum_{i=1}^{n}\left(e_{\exp}-e_{calc}\right)^2}{n}}\cdot 100 \quad (10)$$

The volumetric fraction of broken cells in the BSG, r, was above 0.65 for nearly all of the experiments, except for the lowest pressure at the highest temperatures. The values obtained for the solid-phase mass transfer coefficients, $k_sa_s$, are of the same order than those obtained by Benito-Román et al. (2018) when correlating supercritical extraction data of quinoa oil. The crossing point, $q_c$, was found to increase with a decrease in the solubility value, specially at the lowest operating pressure.

### 3.1.3. Characterization of sc-$CO_2$ extracts

Characterization of the sc-$CO_2$ extracts has been carried out by determining their fatty acid profile, total phenolic and flavonoid content and antioxidant capacity.

A total of 16 fatty acids were identified and quantified in the different sc-$CO_2$ extracts (Table S2 and Fig. S2). No trend in the fatty acid percentage profile was observed neither with the extraction pressure nor with extraction temperature. In all the extracts, linoleic acid was the major fatty acid (>50%), followed by palmitic and oleic acid. Table S2 also includes the fatty acid profile for BSG oil obtained by

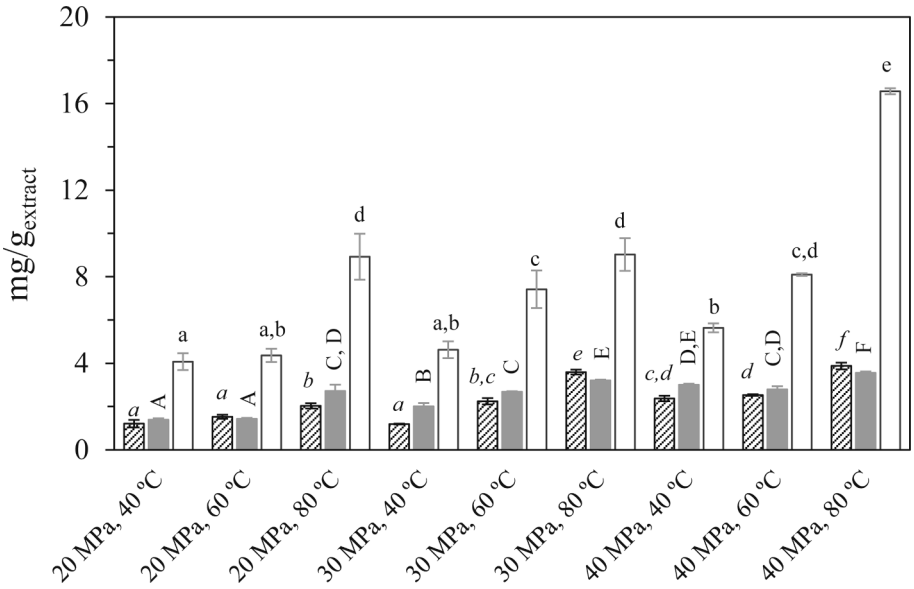


**Fig. 3.** Characterization of sc-$CO_2$ extracts of BSG at different operating conditions: (▨) total flavonoid compounds, mg QE/$g_{extract}$; (▩) antioxidant capacity, mg TE/$g_{extract}$; (□) total phenolic compounds, mg GAE/$g_{extract}$. Values with different letters for each type of measurement (TPC, TFD and antioxidant capacity) are significantly different when applying the Fisher's least significant differences (LSD) method at p-value ≤ 0.05.

Soxhlet extraction. Fărcaş et al. (Fărcaş et al., 2015) reported similar fatty acid composition of BSG by extracting the total lipids using a chloroform:methanol mixture.

The sc-$CO_2$ extracts were also analyzed in terms of total phenolic and flavonoid compounds and antioxidant capacity (Fig. 3). Temperature and pressure significantly affect the three parameters. Extracts obtained at higher pressures resulted in higher content of TPC, TFC and antioxidant activity, although the effect of pressure was less significant than the effect of temperature. The results of the statistical analysis are also presented in Fig. 3. Temperature presented the main effect, specially at the highest pressure studied in this work. In literature, the effect of temperature on the solubility of some phenolic compounds was reported to be negative at low pressure, between 10 and 15 MPa (Murga et al., 2003). However, at higher pressures (>15 MPa), the temperature had a positive effect, as it has been also observed in this work. This behavior was due to the increase in vapour pressure of the solute with temperature that compensate the decrease in $CO_2$ density with temperature. The positive effect of temperature in the pressure range covered in this work was observed for both, TPC and TFC. The increase observed in TPC and TFC led to an increase of the antioxidant capacity of the extracts. It must be highlighted that different crossover point was observed for the bioactive compounds and for the extracted oil, where the crossover point was around 40 MPa.

Ferrentino et al. (Ferrentino et al., 2019) reported the TPC content and the antioxidant capacity, evaluated through the DPPH test, at two levels of pressure and temperature (20/30 MPa and 40/50 °C), with maximum values of 8.4 ± 0.1 mg GAE/$g_{sample}$ and 4.3 ± 0.1 mg Trolox/$g_{sample}$ at 30 MPa and 50 °C, similar to the values plotted in Fig. 3. These authors reported also composition data when using ethanol as co-solvent, 4 and 8%, with maximum values of bioactive compounds of 26.2 ± 0.3 mg GAE/$g_{sample}$ and 14.2 ± 0.1 mg Trolox/$g_{sample}$ at 30 MPa, 50 °C and 8% ethanol. Spinelli et al. (2016) studied the influence of the sc-$CO_2$ operating conditions on the TPC, TFC and the AA, determined as the inhibition percentage of the DPPH radical of the sc-$CO_2$ extracts, focusing on the addition of ethanol as cosolvent. These authors concluded that, in the case of sc-$CO_2$ without co-solvent, the pressure barely had an effect on the chemical composition in the temperature and pressure range from 40 to 60 °C and 15 to 35 MPa, respectively. According to these authors the BSG contains many polar substances with low solubility in pure sc-$CO_2$, concluding that it is necessary to add ethanol to increase the polarity of the extraction solvent. They found that the best operating conditions were 40 °C, 35 MPa and 60% ethanol as co-solvent (v/v) with values of 0.35 ± 0.01 mg GAE/$g_{BSG}$ (4.3 mg GAE/$g_{extract}$), 0.22 ± 0.01 mg QE/$g_{BSG}$ (2.7 mg QE/$g_{extract}$) and 2.09 ± 0.04% of DPPH inhibition. It must be highlihted that in the work of Spinelli et al. (2016) the ethanol concentration is much more higher than the concentration usually employed of ethanol as modifier in sc-$CO_2$ extraction (Ferrentino et al., 2019). In fact, 60% of ethanol concentration would be similar to an ethanolic extraction that should have reached higher TPC yield according to pervious literature data on TPC extraction by ethanolic mixtures (Alonso-Riaño et al., 2020). In the present work, the best conditions in terms of chemical composition were 80 °C and 40 MPa with values of 16.6 mg GAE/$g_{extract}$ (0.94 ± 0.01 mg GAE/$g_{BSG}$), 3.88 mg QE/$g_{extract}$ (0.219 ± 0.009 mg QE/$g_{BSG}$) and 3.56 mg TE/$g_{extract}$ (0.201 ± 0.003 mg Trolox/$g_{BSG}$). The results of bioactive compounds reported in this work, as well as those reported in literature, should be considered with skepticism, as suggested by Guido and Moreira (2017), since conclusions are obtained from spectrophotometric analysis and individual bioactive compounds were not determined. Futhermore, analysis protocols for TPC, TFC and AA were different among the different reported works. Kitryté et al. (2015) redissolve the sc-$CO_2$ in *n*-hexane, while Spinelli et al. (2016) and Ferrentino et al. (2019) dissolved the sc-$CO_2$ extract in ethanol, but at concentrations higher than in this work and higher than the range of solubility of oil in ethanol.

Regarding chemical composition of the lipid fraction of BSG, Guido and Moreira (2017) concluded that typical hydroxycannamic acids present in the BSG, such as ferulic and p–coumaric acids were almost negligible in the extracts obtained by sc-$CO_2$ and ethanol as co-solvent, concluding that essential oils accounted for 13% of oil fraction that contribute for its antioxidant activity. Bohnsack et al. (2011) found tocotrienols and tocopherols in the extracting oil from BSG, specially in the sieving fraction of particle sizes <500 μm. Series of 5-*n*-alkylresorcinols, as well as different classes of steroid compounds have been also identified among the lipids in BSG with antioxidant activity (del Río et al., 2013).

### 3.2. Enzymatic hydrolysis

After sc-$CO_2$ treatment, the raffinate obtained at 40 MPa and 80 °C

was subjected to enzymatic hydrolysis by cellulase at different enzyme doses. As control, the non-sc-$CO_2$ treated BSG was also enzymatically hydrolyzed at the same conditions. At the sc-$CO_2$ extraction conditions studied in this work, the weight loss of the initial raw material corresponds to the lipophilic fraction extracted by the sc-$CO_2$ material (a medium value of 5.7% of weight loss), and the content of other components was not affected after sc–$CO_2$ extraction conditions. Therefore, the carbohydrate fraction remained in the raffinate phase after extraction (Table S3). A similar finding was obtained by Taheri et al. (2021) in the study of the effect of the pretreatment technique on enzymatic hydrolysis of food wastes after Soxhlet solid–liquid fat extraction.

Fig. 4a represents the glucose concentration along enzymatic hydrolysis for sc-$CO_2$ treated BSG and non-treated at different enzyme concentrations. This Figure also shows the glucose concentration in the liquid extract carried out at the same conditions (acetate buffer and 50 °C), but with no enzyme addition. It is clear that glucose was not released to the medium in the absence of enzyme. Comparison of enzymatic performance for sc-$CO_2$ treated and non-treated BSG was done at different cellulose doses in a BSG dry basis. However, after removal of the fat content, the percentage of glucan content in the sc-$CO_2$ treated in a dry basis was higher than in the untreated BSG what means slightly lower enzyme:glucans ratios for the sc-$CO_2$ treated BSG. To better compare results in terms of enzyme dose in a glucan basis, initial reaction rate for all the experiments was evaluated and plotted as a function of the enzyme concentration in a glucan basis (Fig. 4b). Higher values of the slope indicate higher initial reaction rates for sc-$CO_2$ treated BSG than for untreated. An ANOVA confirmed statistically significant differences among the slopes at the 95% confidence level and among the intercepts at the 99% confidence level.

At the end of the enzymatic hydrolysis, statistically significant higher glucose concentration in the medium was obtained for sc-$CO_2$ treated BSG compared to non-treated BSG for all the enzymes concentrations. The percentage increase in glucose concentration evaluated at the end of the experimental extraction curves, for sc-$CO_2$ treated and non-treated BSG was 20, 18 and 17% for the three cellulase concentrations essayed in this work, 0.25, 0.5 and 1%, respectively. This percentage increase was similar to the value reported by Gao et al. (2010) for the enzymatic hydrolysis of sc-$CO_2$ treated and non-treated rice straw with a mixture of cellulase and β-glucosidase. These authors obtained a final glucose yield of 32.4% for sc-$CO_2$ pretreated rice straw at 30 MPa and 110 °C during 30 min compared with 27.7% of glucose yield for non-pretreated rice straw, after 48 h of enzymatic treatment. That meant a percentage increase of about 17%.

Morais et al. (2015) reviewed the use of carbon dioxide in biomass processing by considering the sc-$CO_2$ not only as an extraction medium but also as an agent to pretreat the biomas for subsequent enzymatic hydrolysis of the polysaccharides. According to different studies, it was shown that to obtain high yield of reducing sugars, the most important parameters were the temperature and the moisture content. For instance, Narayanaswamy et al. (2011) observed that for wet corn stover (75%, w/w) at 24 MPa, 120 °C for 60 min, the glucose yield was double compared to dry raw material. Kim & Hong (2001) also reported that a certain content of moisture was needed in the treatment of hardwood and softwood lignocellulosic materials to observe an improvement in enzymatic hydrolysis after sc-$CO_2$ biomass pretreatment. A 57% moisture content resulted in a 77 ± 3 and 37 ± 2% reducing sugar yield for aspen and southern yellow pine, respectively, compared to 15 ± 2 and 13 ± 3% for untreated biomass. As reported by Morais et al. (2015) water can exert a double effect; on one hand, water facilitates a swelling effect on biomass, but also the presence of $CO_2$ acidifies the aqueous medium, causing a similar effect as a dilute-acid hydrolysis. In any case, physical properties of pressurized water at the operating conditions in previous reported studies play an important role in the improvement of enzymatic digestibility after treatment of the biomass in pressurized

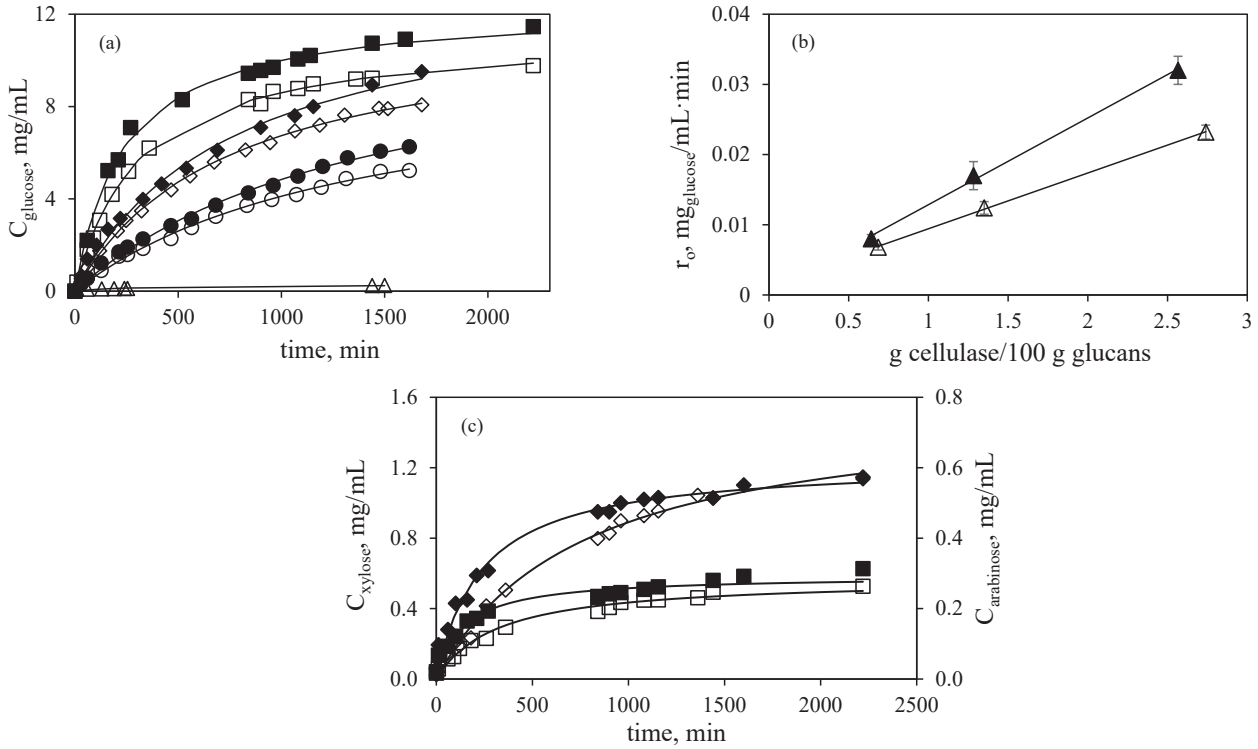


**Fig. 4.** Results of enzymatic hydrolysis at 50 °C (a) Glucose monomer concentration by using different cellulase dose in a BSG dry basis: (△) no cellulase; (○, ●) 0.25% cellulase; (◆, ◇) 0.5% cellulase; (□, ■) 1% cellulase. (b) Initial reaction rates for glucose release at different cellulase dose in a substrate (glucan) base (△, ▲); (c) (◆, ◇) xylose monomer concentration (□, ■) arabinose monomer concentration at 1% of cellulase dose in a BSG dry basis. Open symbols: untreated BSG. Filled symbols: sc-$CO_2$ treated BSG. Continuous lines: in (a) and (c) represent the Holtzapple model in (b) the linear regression: for sc-$CO_2$ treated BSG, $r_o = 0.0124\ E + 0.0005$ $R^2 = 0.9978$; for untreated BSG, $r_o = 0.0079\ E + 0.0015$ $R^2 = 0.9996$ (E = cellulase dose in a glucan basis).

water-$CO_2$ systems. In fact, as reported by Morais et al. (2014) after treatment at 130 °C with $CO_2$ in the medium (up to 3 MPa), the subsequent glucose yield after enzymatic hydrolysis was 39.97% after 96 h, only slightly higher than for untreated material that yielded 34.31% (around 17% increase, similar to the enhancement obtained in this study). On the contrary, in presence of only pressurized water, with no $CO_2$ in the medium, 75% of the hemicellulose from wheat straw was removed at 180 °C. And, according to Aguirre-Fiero et al. (2020) improvement of enzymatic saccharification of cellulose after treatment in pressurized systems water-$CO_2$ was due to an effective hemicellulose removal. Hemicellulose extraction by hydrothermal treatments is one of the most promising options since relative mild temperatures (160–210 °C) are required due to the properties of pressurized water under these conditions such as an increase in the ionic product that favors ionic reactions.

Therefore, it can be clearly observed that more severe conditions were employed in these previous works than the usual temperature range employed for sc-$CO_2$ extraction of the oil fraction from different vegetables matrix. Although water and high temperatures are encouraged to improve the subsequent enzymatic yield, in this work BSG was dried before sc-$CO_2$ extraction and the maximum operating temperature was 80 °C. Higher temperature would led to oxidation of the extracted oil. Furthermore, by increasing water content in the feedstock, some water will be co-extracted with BSG oil and the extraction would be not so efficient. As described in literature (Dunford & Temelli, 1997) for cooked and preheated canola samples, water coextraction led to milky droplets in the oil when the initial moisture content was higher than 12% and the cloudiness of extracts could be correlated with moisture loss from feed material. Therefore, drying of the BSG was carried out before sc-$CO_2$ extraction to obtain an oily fraction of good quality. This way, the sc-$CO_2$ treatment carried out in this work, offers the advantage of obtaining an added-value oily product as extract in addition to the improvement of subsequent enzymatic hydrolysis. Furthermore, the presence of lipids during enzymatic hydryolysis could cause different problems such as clogging, flotation, and mass transfer issues inside the reactor (Taheri et al., 2021). In any case, the improvement of enzymatic digestibility would also depend on biomass composition.

At 1% of cellulase dose, the hydrolysis kinetics for xylose and arabinose have been also determined for non-treated and sc-$CO_2$ treated BSG (Fig. 4c). Higher initial reaction rates were obtained for sc-$CO_2$-treated BSG compared to non-treated BSG. Although not big differences were observed in the final sugar concentration in the hydrolysates. The fitted parameters of Eq. (7), $C_{i,max}$ and $t_{1/2}$ for non-treated and sc-$CO_2$ treated BSG are shown in Table S4. According to Fig. 4, higher values of $C_{i,max}$ for glucose were obtained for sc-$CO_2$ treated BSG. At the highest enzyme dose essayed in this work, the reduction in $t_{1/2}$ was 23% for sc-$CO_2$-treated BSG compared to non-treated-BSG. For xylose and arabinose, the final extraction yield was similar for non-treated and sc-$CO_2$ treated BSG, but $t_{1/2}$ decreased for the sc-$CO_2$ treated BSG (69 and 55% for xylose and arabinose, respectively). The calculated hydrolysis curves are plotted in Fig. 4a and 4c where a good agreement can be observed between experimental data and the model.

BSG is a lignocellulosic biomass but it is also a valuable source of phenolic compounds, being hydroxycinnamic acids, such as ferulic and p-coumaric acids, the primary class of phenolic compounds. Enzyme assisted extraction of phenolic compounds is a suitable technology to achieve good extraction yields of these bioactive compounds. In this work, some phenolic compounds were determined in the enzymatic hydrolysates at the end of the hydrolysis by using 1% of cellulase. Table 1 summarizes the values obtained in this work, together with other values previously reported by alkaline and enzymatic hydrolysis by using 1% xylanase and subcritical water hydrolysis (Alonso-Riaño et al., 2021; Alonso-Riaño et al., 2020). The concentration of p-coumaric and vanillin after cellulase hydrolysis was lower than the values previously reported for the same BSG by xylanase (1%), alkaline hydrolysis and subcritical water hydrolysis. However for ferulic acid, only alkaline hydrolysis provided a higher value. Comparing the different results for cellulase treatment of non-treated and sc-$CO_2$ treated BSG, it can be observed that for vanillin similar concentration in the hydrolysates was obtained for both sustrates. However for p-coumaric acid and ferulic acid, a concentration 31% and 24% higher, respectively, was obtained in the BSG cellulase hydrolysates after sc-$CO_2$ treatment. That proves that sc-$CO_2$ treatment was also effective in the subsequent release of phenolic compounds.

### 3.3. Mechanisms of enzymatic hydrolysis improvement after sc-$CO_2$ treatment

The higher enzymatic hydrolysis rate and yield obtained in the sc-$CO_2$ treated BSG compared with the untreated BSG could be partially attributed to the removal of the lipid fraction. As it has been described in literature (Taheri et al., 2021), fats and oils could influence the susceptibility of carbohydrates to enzymes. Hu et al. (2018) reported that the removal of lipids improved the enzymatic hydrolysis of starch by accelerating the penetration of enzymes into the starch granules and increasing the adsorption of enzymes to its substrate. Munira et al. (2018) indicated that the lipid and protein, together with starch, might inhibit the enzymatic hydrolysis of starch as it was demonstrated by adding different fatty acids to starch and performing a subsequent enzymatic hydrolysis process by α-amylase and amyloglycosidase enzymes. Therefore, it could be assumed an inhibition of cellulase enzymatic hydrolysis due to the presence of lipids. In this regard, Taheri et al. (2021) concluded that the removal of fat by Soxhlet solid liquid extraction was the most appropriate pretreatment to increase the sugar yield by enzymatic hydrolysis for food waste collected from households, among different pretreatments essayed such as hydrothermolysis, sonolysis, electrocatalysis, electrolysis and sono-electrolysis.

The structural and chemical changes among untreated, sc-$CO_2$ treated and hydrolysed BSG were assessed by scanning electron microscopy and X-ray powder diffraction.

#### 3.3.1. Scanning electron microscope observation of BSG structure.

The morphological changes of BSG after sc-$CO_2$ and enzymatic hydrolysis treatments were determined by scanning electron microscopy (SEM) (Fig. 5). The untreated BSG presented a more rigid and continuous surface than after enzymatic and sc-$CO_2$ treatment at 40 MPa and 80 °C. After sc-$CO_2$ treatment, the BSG exhibited an irregular porosity and lamellar structure. sc-$CO_2$ breaks partially some structural barriers allowing a better enzyme access yielding higher hydrolysis yied. Gao et al. (2010) also reported that microfibrils of rice straw were separated form the initial connected structure after sc-$CO_2$ at 30 MPa and 110 °C improving the enzyme access after treatment. From the micrographs of

**Table 1**
Phenolic compounds release yield by different treatments.

| Treatment | p-coumaric acid μg/$g_{BSG}$ | Vanillin μg/$g_{BSG}$ | Ferulic acid μg/$g_{BSG}$ | Reference |
|---|---|---|---|---|
| Celullase, 1% | 3.0 ± 0.3 | 20 ± 1 | 274 ± 4 | This work |
| sc-$CO_2$ + Celullase, 1% | 3.9 ± 0.3 | 21 ± 2 | 341 ± 6 | This work |
| Xylanase, 1% | 6 ± 1 | 111 ± 3 | 52.4 ± 0.9 | (Alonso-Riaño et al., 2021; Alonso-Riaño et al., 2020) |
| Alakaline hydrolysis | 538 ± 4 | 217 ± 1 | 1305.7 ± 0.5 | |
| Subcritical water, 185 °C | 60 ± 8 | 330 ± 11 | 144 ± 10 | |

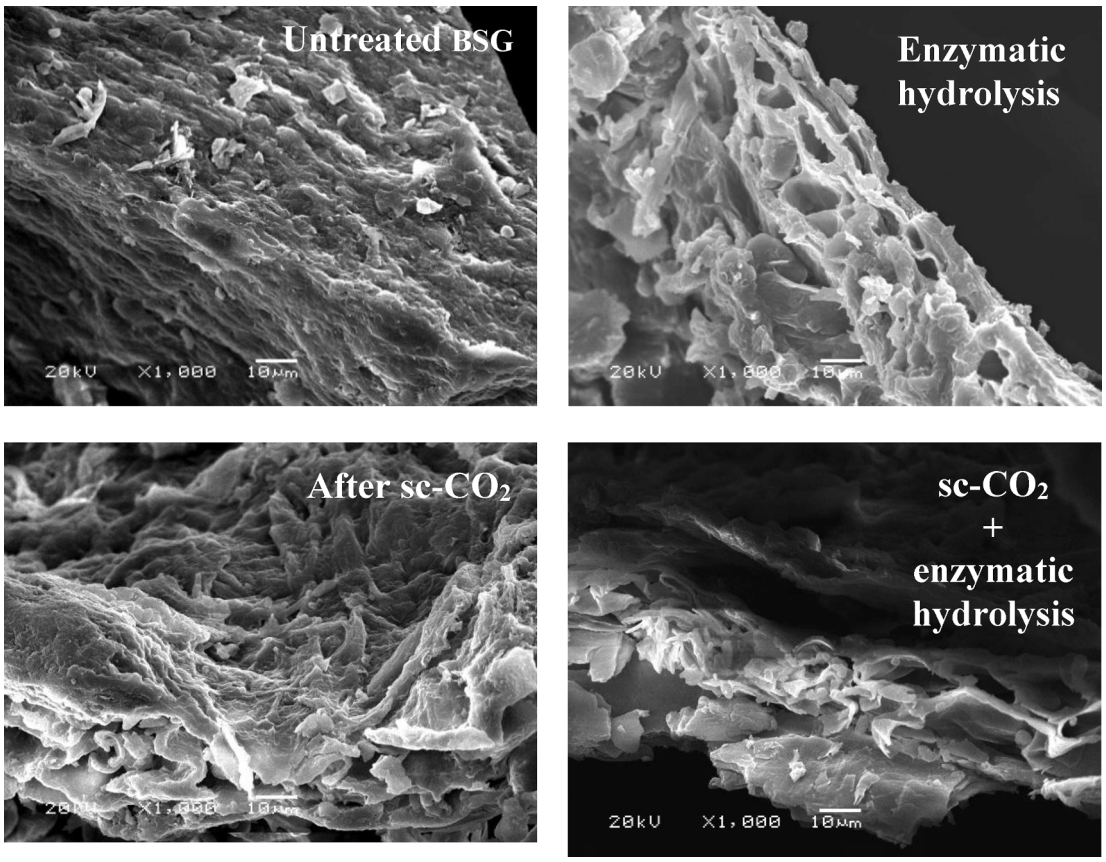


**Fig. 5.** SEM micrographs (1000 × magnifications) of the different BSG samples: untreated BSG, sc-$CO_2$ treated BSG and after enzymatic hydrolysis.

the enzymatic hydrolyzed BSG, it can be seen that the enzymatic hydrolysis left a swollen structure, with a porous and irregular structure, more disgregated in the case of the previously sc-$CO_2$ treated BSG. This might be an indication of the intensity of the process and the removal of soluble and hydrolysable compounds.

### 3.3.2. *X-ray powder diffraction (XRD) analysis*

The XRD patterns of original BSG and the BSG after sc-$CO_2$ and enzymatic hydrolysis treatments is presented in Fig. S3. The diffractogram for untreated BSG presented a broad peak at 21.6° and a small peak at 34.6°. A similar XRD pattern for raw BSG has been reported in literature (Michelin & Teixeira, 2016; Mishra et al., 2017). Based on the XRD curve for BSG the crystallinity index as proposed by Segal et al. for native cellulose (Segal et al., 1959) was not evaluated in this work since the typical 0 0 2 lattice diffraction scattered intensity at the main peak around 22.5° for cellulose I was not observed. The lack of the typical crystalline and amorphous peaks at 22.5° and 18°, respectively was also indicated by Michelin and Teixeira (2016) in the study of the degree of crystallinity of different bio-based materials. However, other authors (Mishra et al., 2017) evaluated the crystallinite index for untreated BSG according to Segal et al. (1959) obtaining a crystallinity index of 17.4% (in the present work a crystallinity index of 16.6% would have been obtained). The XRD pattern for BSG can be explained considering the BSG chemical composition with important amounts of different biopolymers, mainly proteins, hemicellulose, lignin, etc., which influence the XRD pattern (Michelin & Teixeira, 2016). Therefore, its structure is supposed to be semi-crystalline with broad bands and with a highly unclear crystallinity index as it can be observed in Fig. S3.

After sc-$CO_2$ treatment a peak appeared at 26.6° and the peak at 34.7° was more remarkable. The XRD pattern after sc-$CO_2$ treatment indicated that the pretreatment was not strong enough to modify the BSG crystallinity. Narayanaswamy et al. (2011) observed no change in crystallinity when comparing sc-$CO_2$ treated and untreated corn stover, probably due to the complex structure of corn stover where cellulose microfibrils are embedded in hemicellulose, lignin and glycoproteins. Similar findings were reported by Liu et al. (Liu et al., 2014) for cornstalk and rice stray. These authors concluded that a change in biomass crystallinity might not be the only factor that could influence the enzymatic hydrolysis of the biomass. In any case, Park et al. (2010) indicated that the interpretation of data on cellulose hydrolysis by enzymes in terms of cristallynity, assuming that the easily-accessible amorphous regions are more rapidly digested than the more difficult crystalline, is not straightforward based on several reasons, such as not a clear trend found in literature regarding the crystalline index and the hydrolysis degree. The effect of other components, such as particle size and porosity of the native cell wall sample must be considered.

After enzymatic hydrolysis, crystallinity seemed to increase based on the XRD plot with a sharper main peak and diffraction angles at around 34.7° for both untreated and sc-$CO_2$ treated BSG, probably due to the digestion of the amorphous cellulose fraction of the BSG during the enzymatic hydrolysis.

## 4. Conclusions

sc-$CO_2$ has a double effect in a biorefinery context to include the BSG into a circular economy concept: (1) as green solvent for oil recovery obtaining an oily extract rich in linoleic acid with important amounts of bioactive compounds that provide good antioxidant properties (2) as pretreatment agent for further improvement of the enzymatic hydrolysis yield of the sc-$CO_2$ treated BSG. This improvement was mainly due to surface morphology modification and lipid fraction removal that facilitates the access of the enzymes. sc-$CO_2$ extraction led to an increase in sugar release of approximately 20% compared to the non-treated BSG. The increase in sugar production will enhance subsequent

biotechnological process.

Therefore in this work, low value BSG has been incorporated within a circular economy concept to obtain a valuable oil fraction and a useful residue for further hydrolytic enzyme process.

## Funding

This work was supported by the Agencia Estatal de Investigación [grant number PID2019-104950RB-I00 / AEI / https://doi.org/10.13039/501100011033] and the Junta de Castilla y León (JCyL) and the European Regional Development Fund (ERDF) [grant numbers BU301P18 and BU050P20]. E. Trigueros and P. Alonso-Riaño predoctoral contracts were funded by JCyL and the European Social Fund (ESF) by *ORDEN EDU/574/2018*, de 28 de mayo and *ORDEN EDU/556/2019, de 5 de junio, respectively*.

*CRediT authorship contribution statement*

**P. Alonso-Riaño:** Investigation, Methodology, Writing – original draft. **Rodrigo Melgosa:** Formal analysis, Writing – original draft. **E. Trigueros:** Formal analysis. **A.E. Illera:** Formal analysis. **Sagrario Beltrán:** Resources, Funding acquisition, Conceptualization. **M. Teresa Sanz:** Writing – original draft, Conceptualization, Project administration, Resources.

## Declaration of Competing Interest

The authors declare that they have no known competing financial interests or personal relationships that could have appeared to influence the work reported in this paper.

## Data availability

Data will be made available on request.

## Acknowledgment

The authors acknowledge Brebajes del Norte for kindly providing the BSG used in this work.

## Appendix A. Supplementary data

Supplementary data to this article can be found online at https://doi.org/10.1016/j.foodchem.2022.133493.

## References

Aguirre-Fierro, A., Ruiz, H. A., Cerqueira, M. A., Ramos-González, R., Rodríguez-Jasso, R. M., Marques, S., & Lukasik, R. M. (2020). Sustainable approach of high-pressure agave bagasse pretreatment for ethanol production. *Renewable Energy, 155*, 1347–1354. https://doi.org/10.1016/j.renene.2020.04.055

Alonso-Riaño, P., Sanz, M. T., Benito-Román, O., Beltrán, S., & Trigueros, E. (2021). Subcritical water as hydrolytic medium to recover and fractionate the protein fraction and phenolic compounds from craft brewer's spent grain. *Food Chemistry, 351*. https://doi.org/10.1016/j.foodchem.2021.129264

Alonso-Riaño, P., Sanz Diez, M. T., Blanco, B., Beltrán, S., Trigueros, E., & Benito-Román, O. (2020). Water ultrasound-assisted extraction of polyphenol compounds from Brewer's spent grain: Kinetic study, extract characterization, and concentration. *Antioxidants, 9*(3), 265. https://doi.org/10.3390/antiox9030265

AOAC. (1997). *Tittle Fatty acids in oils and fats. Preparation of methyl esters boron trifluoride method AOAC 969.33-1969(1997), Fatty acids in oils and fats. 1969*, 1997.

Arshadi, M., Attard, T. M., Lukasik, R. M., Brncic, M., Da Costa Lopes, A. M., Finell, M., … Yuste-Córdoba, F. J. (2016). Pre-treatment and extraction techniques for recovery of added value compounds from wastes throughout the agri-food chain. *Green Chemistry, 18*(23), 6160–6204. https://doi.org/10.1039/c6gc01389a

Benito-Román, O., Rodríguez-Perrino, M., Sanz, M. T., Melgosa, R., & Beltrán, S. (2018). Supercritical carbon dioxide extraction of quinoa oil: Study of the influence of process parameters on the extraction yield and oil quality. *Journal of Supercritical Fluids, 139*(May), 62–71. https://doi.org/10.1016/j.supflu.2018.05.009

Bohnsack, C., Ternes, W., Büsing, A., & Drotleff, A. M. (2011). Tocotrienol levels in sieving fraction extracts of brewer's spent grain. *European Food Research and Technology, 232*(4), 563–573. https://doi.org/10.1007/s00217-010-1419-z

Bucić-Kojić, A., Sovová, H., Planinić, M., & Tomas, S. (2013). Temperature-dependent kinetics of grape seed phenolic compounds extraction: Experiment and model. *Food Chemistry, 136*(3–4), 1136–1140. https://doi.org/10.1016/j.foodchem.2012.09.087

del Río, J. C., Prinsen, P., & Gutiérrez, A. (2013). Chemical composition of lipids in brewer's spent grain: A promising source of valuable phytochemicals. *Journal of Cereal Science, 58*(2), 248–254. https://doi.org/10.1016/j.jcs.2013.07.001

Del Valle, J. M., De La Fuente, J. C., & Uquiche, E. (2012). A refined equation for predicting the solubility of vegetable oils in high-pressure CO 2. *Journal of Supercritical Fluids, 67*, 60–70. https://doi.org/10.1016/j.supflu.2012.02.004

Dunford, N. T., & Temelli, F. (1997). Extraction conditions and moisture content of canola flakes as related to lipid composition of supercritical CO2 extracts. *Journal of Food Science, 62*(1), 155–159. https://doi.org/10.1111/j.1365-2621.1997.tb04389.x

Fărcaș, A. C., Socaci, S. A., Dulf, F. V., Tofană, M., Mudura, E., & Diaconeasa, Z. (2015). Volatile profile, fatty acids composition and total phenolics content of brewers' spent grain by-product with potential use in the development of new functional foods. *Journal of Cereal Science, 64*, 34–42. https://doi.org/10.1016/j.jcs.2015.04.003

Fernández, M. P., Rodriguez, J. F., García, M. T., De Lucas, A., & Gracia, I. (2008). Application of supercritical fluid extraction to brewer's spent grain management. *Industrial and Engineering Chemistry Research, 47*(5), 1614–1619. https://doi.org/10.1021/ie0708529

Ferrentino, G., Ndayishimiye, J., Haman, N., & Scampicchio, M. (2019). Functional activity of oils from Brewer's spent grain extracted by supercritical carbon dioxide. *Food and Bioprocess Technology, 12*(5), 789–798. https://doi.org/10.1007/s11947-019-02249-3

Gao, M., Xu, F., Li, S., Ji, X., Chen, S., & Zhang, D. (2010). Effect of SC-CO2 pretreatment in increasing rice straw biomass conversion. *Biosystems Engineering, 106*(4), 470–475. https://doi.org/10.1016/j.biosystemseng.2010.05.011

Guido, L. F., & Moreira, M. M. (2017). Techniques for extraction of Brewer's spent grain polyphenols: A review. *Food and Bioprocess Technology, 10*(7), 1192–1209. https://doi.org/10.1007/s11947-017-1913-4

Holtzapple, M. T., Caram, H. S., & Humphrey, A. E. (1984). A comparison of two empirical models for the enzymatic hydrolysis of pretreated poplar wood. *Biotechnology and Bioengineering, 26*(8), 936–941. https://doi.org/10.1002/bit.260260818

Hu, P., Fan, X., Lin, L., Wang, J., Zhang, L., & Wei, C. (2018). Effects of surface proteins and lipids on molecular structure, thermal properties, and enzymatic hydrolysis of rice starch. *Food Science and Technology, 38*(1), 84–90. https://doi.org/10.1080/10942912.2018.1561464

Kim, K. H., & Hong, J. (2001). Supercritical CO2 pretreatment of lignocellulose enhances enzymatic cellulose hydrolysis. *Bioresource Technology, 77*(2), 139–144. https://doi.org/10.1016/S0960-8524(00)00147-4

Kitryte, V., Šaduikis, A., & Venskutonis, P. R. (2015). Assessment of antioxidant capacity of brewer's spent grain and its supercritical carbon dioxide extract as sources of valuable dietary ingredients. *Journal of Food Engineering, 167*, 18–24. https://doi.org/10.1016/j.jfoodeng.2014.12.005

Liu, Y. F., Luo, P., Xu, Q. Q., Wang, E. J., & Yin, J. Z. (2014). Investigation of the effect of supercritical carbon dioxide pretreatment on reducing sugar yield of lignocellulose hydrolysis. *Cellulose Chemistry and Technology, 48*(1–2), 89–95.

Manzanares, P. (2020). The roble of biorefinering research in the development of a modern bioeconomy. *Acta Innovations, 37*, 47–56.

Michelin, M., & Teixeira, J. A. (2016). Liquid hot water pretreatment of multi feedstocks and enzymatic hydrolysis of solids obtained thereof. *Bioresource Technology, 216*, 862–869. https://doi.org/10.1016/j.biortech.2016.06.018

Mishra, P. K., Gregor, T., & Wimmer, R. (2017). Utilising brewer's spent grain as a source of cellulose nanofibres following separation of protein-based biomass. *BioResources, 12*(1), 107–116. https://doi.org/10.15376/biores.12.1.107-116

Morais, A. R. C., Da Costa Lopes, A. M., & Bogel-Łukasik, R. (2015). Carbon dioxide in biomass processing: Contributions to the green biorefinery concept. *Chemical Reviews, 115*(1), 3–27. https://doi.org/10.1021/cr500330z

Morais, A. R. C., Mata, A. C., & Bogel-Lukasik, R. (2014). Integrated conversion of agroindustrial residue with high pressure CO2 within the biorefinery concept. *Green Chemistry, 16*(9), 4312–4322. https://doi.org/10.1039/c4gc01093k

Munira, Padil, Sarto, & Hidayat, M. (2018). Inhibitor effect (lipid and protein) in starch hydrolysis to produce glucose by using amyloglucosidase. *IOP Conference Series: Earth and Environmental Science, 175*(1). 10.1088/1755-1315/175/1/012022.

Murga, R., Sanz, M. T., Beltrán, S., & Cabezas, J. L. (2003). Solubility of three hydroxycinnamic acids in supercritical carbon dioxide. *Journal of Supercritical Fluids, 27*(3). https://doi.org/10.1016/S0896-8446(02)00265-6

Narayanaswamy, N., Faik, A., Goetz, D. J., & Gu, T. (2011). Supercritical carbon dioxide pretreatment of corn stover and switchgrass for lignocellulosic ethanol production. *Bioresource Technology, 102*(13), 6995–7000. https://doi.org/10.1016/j.biortech.2011.04.052

Park, S., Baker, J. O., Himmel, M. E., Parilla, P. A., & Johnson, D. K. (2010). Cellulose crystallinity index: Measurement techniques and their impact on interpreting cellulase performance. *Biotechnology for Biofuels, 3*, 1–10. https://doi.org/10.1186/1754-6834-3-10

Re, R., Pellegrini, N., Proteggente, A., Pannala, A., Yang, M., & Rice-Evans, C. (1999). Antioxidant Activity Applying an Improved Abts Radical Cation Decolorization Assay. *Free Radical Biology and Medicine, 26*(9), 1231–1237. https://doi.org/10.1016/S0891-5849(98)00315-3

Rebolleda, S., Beltrán, S., Sanz, M. T., González-Sanjosé, M. L., & Solaesa, Á. G. (2013). Extraction of alkylresorcinols from wheat bran with supercritical CO 2. *Journal of Food Engineering, 119*(4), 814–821. https://doi.org/10.1016/j.jfoodeng.2013.07.008

Rebolleda, S., Rubio, N., Beltrán, S., Sanz, M. T., & González-Sanjosé, M. L. (2012). Supercritical fluid extraction of corn germ oil: Study of the influence of process

parameters on the extraction yield and oil quality. *Journal of Supercritical Fluids, 72*, 270–277. https://doi.org/10.1016/j.supflu.2012.10.001

Relvas, F. M., Morais, A. R. C., & Bogel-Lukasik, R. (2015). Kinetic modeling of hemicellulose-derived biomass hydrolysis under high pressure CO2-H2O mixture technology. *Journal of Supercritical Fluids, 99*, 95–102. https://doi.org/10.1016/j.supflu.2015.01.022

Segal, L., Creely, J. J., Martin, A. E., & Conrad, C. M. (1959). An empirical method for estimating the degree of crystallinity of native cellulose using the X-ray diffractometer. *Textile Research Journal, 29*(10), 786–794. https://doi.org/10.1177/004051755902901003

Singleton, V. L., Orthofer, R., & Lamuela-Raventós, R. M. (1999). Analysis of total phenols and other oxidation substrates and antioxidants by means of folin-ciocalteu reagent. *Methods in Enzymology, 299*, 152–178. https://doi.org/10.1016/j.scienta.2016.11.004

Sovová, H. (2005). Mathematical model for supercritical fluid extraction of natural products and extraction curve evaluation. *Journal of Supercritical Fluids, 33*(1), 35–52. https://doi.org/10.1016/j.supflu.2004.03.005

Spinelli, S., Conte, A., Lecce, L., Padalino, L., & Del Nobile, M. A. (2016). Supercritical carbon dioxide extraction of brewer's spent grain. *Journal of Supercritical Fluids, 107*, 69–74. https://doi.org/10.1016/j.supflu.2015.08.017

Taheri, M. E., Salimi, E., Saragas, K., Novakovic, J., Barampouti, E. M., Mai, S., Malamis, D., Moustakas, K., & Loizidou, M. (2021). Effect of pretreatment techniques on enzymatic hydrolysis of food waste. *Biomass Conversion and Biorefinery, 11*(2), 219–226. https://doi.org/10.1007/s13399-020-00729-7